

# High temperature neutron diffraction studies of phase transformations in $\text{NiCr}_2\text{S}_4$

Paz Vaqueiro,<sup>a</sup> Steve Hull,<sup>b</sup> Bente Lebech<sup>c</sup> and Anthony V. Powell<sup>\*a</sup>

<sup>a</sup>Department of Chemistry, Heriot-Watt University, Riccarton, Edinburgh, UK EH14 4AS.

E-mail: A.V.Powell@hw.ac.uk

<sup>b</sup>Rutherford Appleton Laboratory, ISIS facility, Didcot, Oxfordshire, UK OX11 0QX

<sup>c</sup>Condensed Matter Physics and Chemistry Department, Risø National Laboratory, DK-4000 Roskilde, Denmark

Received 7th June 1999, Accepted 1st September 1999

High temperature structural transformations in  $\text{NiCr}_2\text{S}_4$  have been investigated by neutron powder diffraction *in situ*. At 835(5) °C,  $\text{NiCr}_2\text{S}_4$  undergoes an order–disorder transition from the monoclinic  $\text{Cr}_3\text{S}_4$  structure to a hexagonal cation-deficient NiAs structure. Above the transition temperature, cation vacancies, which at room temperature are ordered in every second cation layer, become statistically distributed between all cation layers. Prior to this structural transition, intralayer disordering of vacancies within the half-occupied layer. This is not sufficiently complete to cause the change to trigonal symmetry which has been reported for binary sulfides.

## Introduction

Many ternary transition metal sulfides of stoichiometry  $\text{M}_3\text{S}_4$  adopt the monoclinic  $\text{Cr}_3\text{S}_4$  structure, which can be derived from a metal-deficient NiAs-type structure. In the NiAs structure, the cations (M) occupy octahedral sites between pairs of hexagonally close packed anion (X) layers, resulting in a stacking sequence XMXMXM. The introduction, in an ordered manner, of cation vacancies to alternate layers along the *c*-axis of the NiAs unit cell gives rise to a range of vacancy-ordered phases of general formula  $\text{M}_x\text{MS}_2$  ( $0 < x < 1$ ). In the  $\text{Cr}_3\text{S}_4$  structure ( $x = 1/2$ ), fully occupied layers alternate with half occupied layers, resulting in a stacking sequence XMXM<sub>0.5</sub>XM and two crystallographically distinct octahe-

dral cation sites (Fig. 1). This vacancy ordering scheme corresponds to a  $\sqrt{3}a \times a$  two-dimensional supercell. Much of our recent work has concerned the structural and physical properties of  $\text{Cr}_3\text{S}_4$  type ternary sulfides,<sup>1</sup> including  $\text{NiCr}_2\text{S}_4$ .<sup>2</sup> These studies<sup>3</sup> have shown that at room temperature,  $\text{NiCr}_2\text{S}_4$  adopts the  $\text{Cr}_3\text{S}_4$  structure, with a cation distribution close to the normal type, in which nickel cations occupy mainly the half-occupied layer whilst chromium cations reside in the fully occupied layer. Moreover, during the course of investigations of  $\text{NiCr}_2\text{S}_4$ , it has been observed that the magnetic properties of this material are dependent on the preparative conditions. Specifically, magnetic susceptibility curves of materials prepared using different rates of cooling from elevated temperatures, exhibit different magnetic history dependence at low temperatures ( $T < 70$  K). These differences are likely to arise from short-range cation–cation interactions, which are sensitive to the degree of cation ordering. Therefore, in an effort to improve our understanding of the physical properties of this material, we have carried out a high temperature structural study of  $\text{NiCr}_2\text{S}_4$  using powder neutron diffraction.

With increasing temperature, the  $\text{Cr}_3\text{S}_4$ -type structure may transform to a  $\text{CdI}_2$ -type phase as a result of intralayer disordering of vacancies within the half-occupied layer. In the  $\text{Cr}_3\text{S}_4$  structure, cations in the fully occupied layer reside in the octahedral site 4(*i*), while cations in the vacancy layer occupy the octahedral site 2(*a*). The vacancy layer also contains a second octahedral site, 2(*d*), which is empty in the ideal  $\text{Cr}_3\text{S}_4$  structure. With the transformation to the  $\text{CdI}_2$  structure, the two octahedral sites in the vacancy layer become equivalent, and vacancies and cations become distributed at random within this layer. Consequently, the  $\text{CdI}_2$  vacancy layer octahedral site has an occupancy of 50%. As illustrated by Fig. 2, this transformation results in the loss of the two-dimensional supercell and a change from  $I2/m$  symmetry to  $P\bar{3}m1$ . The relationships between the monoclinic  $\text{Cr}_3\text{S}_4$  unit cell parameters and the hexagonal  $\text{CdI}_2$  unit cell parameters are  $a_m \approx \sqrt{3}a_h$ ,  $b_m \approx b_h$ , and  $c_m \approx 2c_h$ . At higher temperatures, a second transition may occur as a result of interlayer disordering. This corresponds to the transformation of the  $\text{CdI}_2$ -type phase to a non-stoichiometric cation deficient NiAs phase, with  $P6_3/mmc$  symmetry, in which all octahedral sites are equivalent, and statistical occupancy of cation sites occurs.

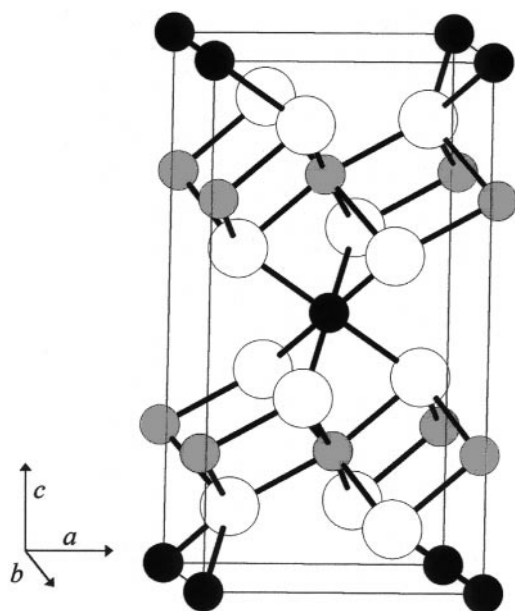
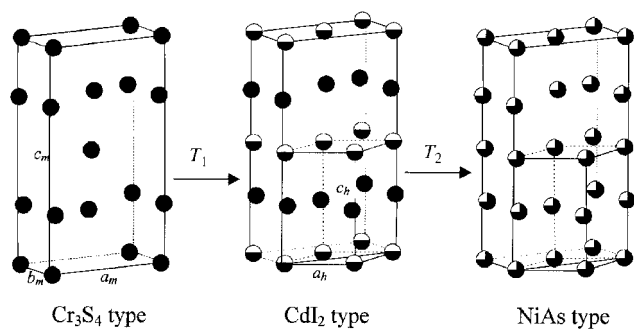


Fig. 1 A ball-and-stick representation of the  $\text{Cr}_3\text{S}_4$  structure. Large open circles represent anions, small black circles represent cations in the vacancy layer and small grey circles represent cations in the fully occupied layer.



**Fig. 2** A schematic model of the structural transformations of the  $\text{Cr}_3\text{S}_4$ -type phase. Anions are omitted for clarity. Black circles represent fully occupied cation sites, half black circles represent a site occupancy of 0.5, and three-quarter black circles represent a site occupancy of 0.75.

Relatively few studies of order–disorder transitions for transition metal chalcogenides with the  $\text{Cr}_3\text{S}_4$  structure have been published. Oka *et al.* determined the phase diagram for the systems  $\text{VS}_x$  and  $\text{VSe}_x$  with  $1.3 \leq x \leq 1.7$ .<sup>4</sup> These authors reported a transformation of  $\text{V}_3\text{X}_4$  from the  $\text{Cr}_3\text{S}_4$  structure to a  $\text{CdI}_2$  phase, with a transition temperature dependent on the stoichiometry, and explained the transition by a statistical thermodynamic treatment.<sup>5,6</sup> Order–disorder transitions have also been reported for the compounds  $\text{Cr}_{3\pm x}\text{Se}_4$ ,<sup>7</sup>  $\text{Cr}_x\text{TiSe}_2$ ,<sup>8</sup>  $\text{Fe}_x\text{VS}_2$ <sup>9</sup> and  $(\text{Fe}_{0.6}\text{V}_{0.4})_{3\pm x}\text{S}_4$ .<sup>10</sup> With the exception of the system  $(\text{Fe}_{0.6}\text{V}_{0.4})_{3\pm x}\text{S}_4$ , only the transformation to the  $\text{CdI}_2$  phase has been observed, although a second transformation to the  $\text{NiAs}$  structure is expected at higher temperatures. Here, we report the results of an investigation in  $\text{NiCr}_2\text{S}_4$  at elevated temperatures, by means of time-of-flight and constant wavelength powder neutron diffraction. A preliminary account of the constant wavelength experiment has been presented at the 2nd European Conference on Neutron Scattering.<sup>11</sup>

## Experimental

The samples were prepared by mixing high-purity nickel, chromium and sulfur powders with the stoichiometry  $\text{NiCr}_2\text{S}_{3.93}$  and firing the mixture in an evacuated silica ampoule at  $800^\circ\text{C}$  for 3 days and at  $1000^\circ\text{C}$  for 9 days with two intermediate regrindings. After the final firing, the products were cooled to  $300^\circ\text{C}$  over a period of 4 h. All reaction mixtures were prepared with a slight deficiency of sulfur, as it has been shown<sup>12</sup> that the phase range of the  $\text{Cr}_3\text{S}_4$  structure does not extend to the fully stoichiometric composition. Details of the preparation and characterisation of the material have been presented elsewhere.<sup>13</sup>

Time-of-flight powder neutron diffraction data were collected on the Polaris diffractometer at the ISIS source, Rutherford Appleton Laboratory. A sample (*ca.* 3 g) was contained in a thin-walled vanadium can which was mounted in a furnace evacuated to a pressure  $< 10^{-4}$  Torr. Data were collected at temperatures in the range  $100 \leq T/^\circ\text{C} \leq 1000$  over intervals of 4 h. At  $900^\circ\text{C}$ , three consecutive data sets were recorded, each over a period of four hours. Preliminary data reduction was carried out using Genie<sup>14</sup> spectrum manipulation software.

Constant wavelength powder neutron diffraction data were recorded on the TAS3 diffractometer at the Risø National Laboratory, Denmark, over the angular range  $10 \leq 2\theta/^\circ \leq 115$  with a wavelength of  $1.54810(7)$  Å. The sample (*ca.* 3 g) was contained in a high-purity boron-free quartz ampoule, which was evacuated, sealed and then mounted in a furnace evacuated to a pressure  $< 10^{-4}$  Torr. Data were collected at room temperature and over the range  $700 \leq T/^\circ\text{C} \leq 870$  in temperature increments of  $10^\circ\text{C}$ . Additional data were collected at 860, 845,  $830^\circ\text{C}$  and room temperature on cooling the sample. Data

collected for the empty furnace were used to provide a background which was subtracted from the room temperature data prior to structural refinement. All Rietveld refinements were carried out using the GSAS package<sup>15</sup> installed on the Heriot-Watt University Alpha 2100-4275 system.

## Results

### Time-of-flight data

Neutron diffraction data, from the highest resolution back-scattering bank of Polaris detectors ( $2\theta = 145^\circ$ ), were summed and normalised. Data from this bank were used in the Rietveld refinements. Over the temperature range  $100 \leq T/^\circ\text{C} \leq 700$  data can be indexed on the basis of the  $\text{Cr}_3\text{S}_4$  monoclinic unit cell. Rietveld refinements were initiated in the space group  $I2/m$  using the structural model determined for this sample at room temperature in an earlier experiment.<sup>3</sup> A region centred at  $d \approx 2.15$  Å was excluded from the refinements owing to the presence of a peak due to vanadium, which is instrumental in origin. With increasing temperature, the monoclinic distortion decreases and above  $700^\circ\text{C}$  data from the highest resolution bank could be satisfactorily indexed either in the space group  $P\bar{3}m1$  or in  $P6_3/mmc$ .

However examination of data from the low angle detector bank ( $2\theta = 35^\circ$ ), which covers a wider range of  $d$ -spacing ( $0.5 < d/\text{Å} < 8.3$ ), revealed that  $(00l)$  reflections with  $l = 2n + 1$  are absent. This indicated that the correct space group is  $P6_3/mmc$ , and all structural refinements using high temperature data above  $700^\circ\text{C}$  were carried out in this space group. Final observed, calculated and difference profiles for the diffraction data collected at 700 and  $800^\circ\text{C}$  are given in Fig. 3. Corresponding refined parameters are shown in Table 1. After cooling the sample to room temperature, a further pattern was recorded, in order to examine the reversibility of the transition. Surprisingly, three phases could be identified in this room temperature pattern: a  $\text{Cr}_3\text{S}_4$ -type phase,  $\text{Ni}$  and  $\text{Ni}_3\text{S}_2$ . A multiphase Rietveld refinement was carried out using these data and the observed, calculated and difference profiles are shown in Fig. 4. Moreover, gradual loss of sulfur at elevated

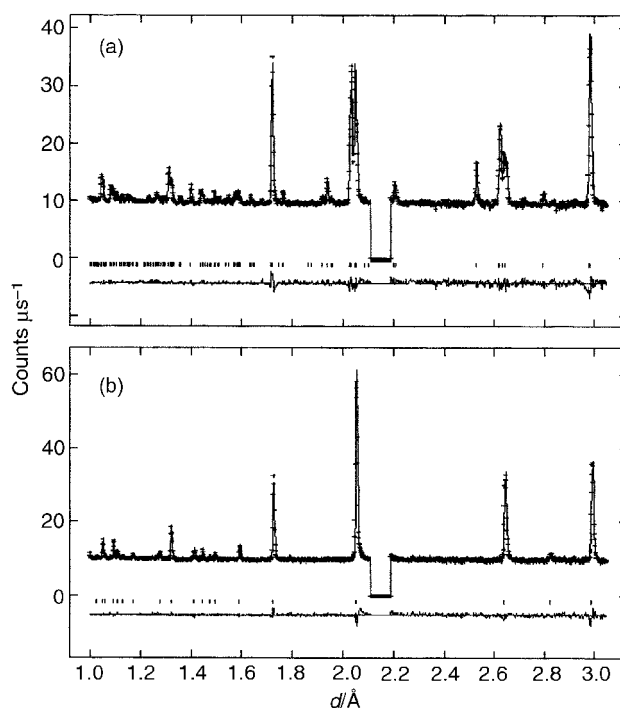


**Fig. 3** Observed (crosses), calculated (upper full line) and difference (lower full line) profiles for data collected on Polaris at (a)  $700^\circ\text{C}$  and (b)  $800^\circ\text{C}$ . Reflection positions are marked.

**Table 1** Final structural parameters derived from Rietveld refinements for NiCr<sub>2</sub>S<sub>4</sub> at high temperature(a) Space group *I2/m*;  $a = 5.9669(2)$  Å,  $b = 3.43943(8)$  Å,  $c = 11.1919(3)$  Å,  $\beta = 90.740(2)^\circ$ 

Temperature 700 °C							
Atom	Site	$x$	$y$	$z$	$B/\text{Å}^2$	SOF	
Ni(1)	2( <i>a</i> )	0.0	0.0	0.0	2.29(7)	0.726(4)	
Cr(1)	2( <i>a</i> )	0.0	0.0	0.0	2.29(7)	0.154	
Ni(2)	2( <i>d</i> )	0.5	0.5	0.0	2.29(7)	0.120(4)	
Ni(3)	4( <i>i</i> )	-0.0206(5)	0.0	0.2611(3)	1.16(7)	0.077	
Cr(3)	4( <i>i</i> )	-0.0206(5)	0.0	0.2611(3)	1.16(7)	0.923	
S(1)	4( <i>i</i> )	0.3288(8)	0.0	0.8767(4)	1.20(6)	0.990(8)	
S(2)	4( <i>i</i> )	0.3383(8)	0.0	0.3654(4)	1.20(6)	0.990(8)	

 $R_{\text{wp}}(\%) = 1.36$ ,  $\chi^2 = 1.28$ (b) Space group *P6<sub>3</sub>/mmc*<sup>a</sup>

Temperature/°C	Instrument	800	845
		Polaris	TAS3
M	$a/\text{Å}$	3.45293(4)	3.4546(2)
	$c/\text{Å}$	5.6488(1)	5.6284(6)
	$B/\text{Å}^2$	2.62(3)	2.0(1)
	SOF Ni	0.258(2)	0.25
S	SOF Cr	0.515(4)	0.5
	$B/\text{Å}^2$	1.63(5)	1.2(1)
	SOF	1.0	1.0
$R_{\text{wp}}(\%)$		1.39	7.6
$\chi^2$		1.35	1.1

<sup>a</sup>M in 2(*a*): (0,0,0); S in 2(*d*): (1/3, 2/3, 1/4).

temperatures was observed and could be followed by structural refinements using data collected at 900 °C over a period of several hours. Despite the constant temperature, lattice parameters resulting from these refinements for which the sample remained at 900 °C, increased as a function of time. Refinement of the site occupancy factors (SOF) indicated an increase in the metal : sulfur ratio, which at 500 °C has the ideal value of 0.75. Above 500 °C, this ratio increases continuously reaching a value of 0.8 at 1000 °C, which corresponds to a composition of NiCr<sub>2</sub>S<sub>3.75</sub>. Standard vanadium cans do not appear to provide a sufficiently good seal and, as the can was contained in a furnace evacuated to high vacuum, the sample composition changed during the course of the experiment. For this reason, these data did not allow the reversibility of the phase transition to be established.

#### Constant wavelength data

Data collected on TAS3 at room temperature were used to refine the structure and establish the cation distribution. Although the cation distribution of the sample used in the TAS3 experiment differs slightly from that used in the Polaris

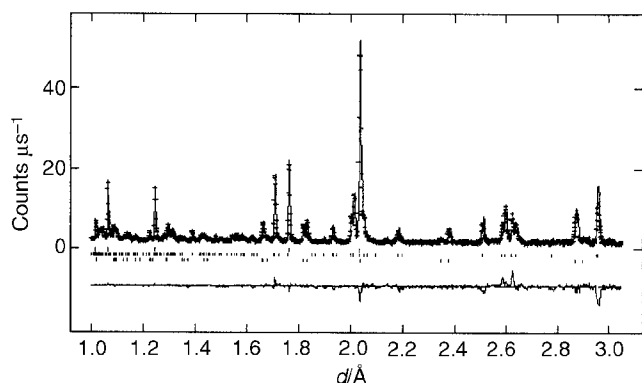


**Fig. 4** Observed (crosses), calculated (upper full line) and difference (lower full line) profiles for the multiphase Rietveld refinement using data collected on Polaris after re-cooling the sample to room temperature. Bottom reflection markers correspond to Ni<sub>3</sub>S<sub>2</sub>, middle markers to a Cr<sub>3</sub>S<sub>4</sub>-type phase and upper markers to Ni.

experiment (7% of Cr in the vacancy layer rather than 15%), both samples have a cation distribution close to the normal type. Refinements carried out using the data collected over the temperature range  $700 \leq T/^\circ\text{C} \leq 830$  were initiated using the structural model determined at room temperature. In these refinements, data over the angular range  $10 \leq 2\theta/^\circ \leq 100$  were used, and those regions in which reflections arising from the furnace were observed, were excluded. The background was modelled by a linear interpolation between fixed points. Diffraction peaks were modelled using a pseudo-Voigt peak shape. Refinement of a scale factor, lattice parameters, atomic positions, peak shape parameters and thermal parameters proceeded smoothly. At this stage, those peaks corresponding to the reflections (-101), (101), (-103), (103) and (310), appeared to be overcalculated in the refinements. These reflections are sensitive to the degree of ordering in the vacancy layer. Therefore Ni cations were introduced to the empty octahedral site 2(*d*), and the site occupancies for both 2(*a*) and 2(*d*) were refined with the constraint that overall stoichiometry be maintained. This improved the agreement between observed and calculated profiles and led to a significant decrease in the weighted residuals. For the data collected over the range  $840 \leq T/^\circ\text{C} \leq 870$  refinements were carried out in the space group *P6<sub>3</sub>/mmc*, corresponding to the NiAs-type structure. Unlike in the Polaris experiment, no loss of sulfur was observed and hence site occupancy factors were not refined. Chromium and nickel cations are statistically distributed in the octahedral site 2(*a*) in a ratio 2 : 1, with an overall site occupancy factor value of 0.75. The final refined parameters for the cation-deficient NiAs phase at 845 °C are given in Table 1. Plots of the lattice parameters, the unit cell volume per formula unit and the site occupancy factor in 2(*d*) are given in Fig. 5, 6 and 7 respectively. With increasing temperature, the unit cell dimensions and the unit cell volume increase whereas the monoclinic angle  $\beta$  decreases from 91.3° at room temperature to 90.6° at 830 °C. Above this temperature, the phase transition takes place and both the unit cell volume and the lattice parameters exhibit a discontinuity. At temperatures close to the phase transition, the data summarised in Fig. 6 show that the unit cell volume on cooling the sample differs slightly from the volume obtained on heating the sample, indicating a degree

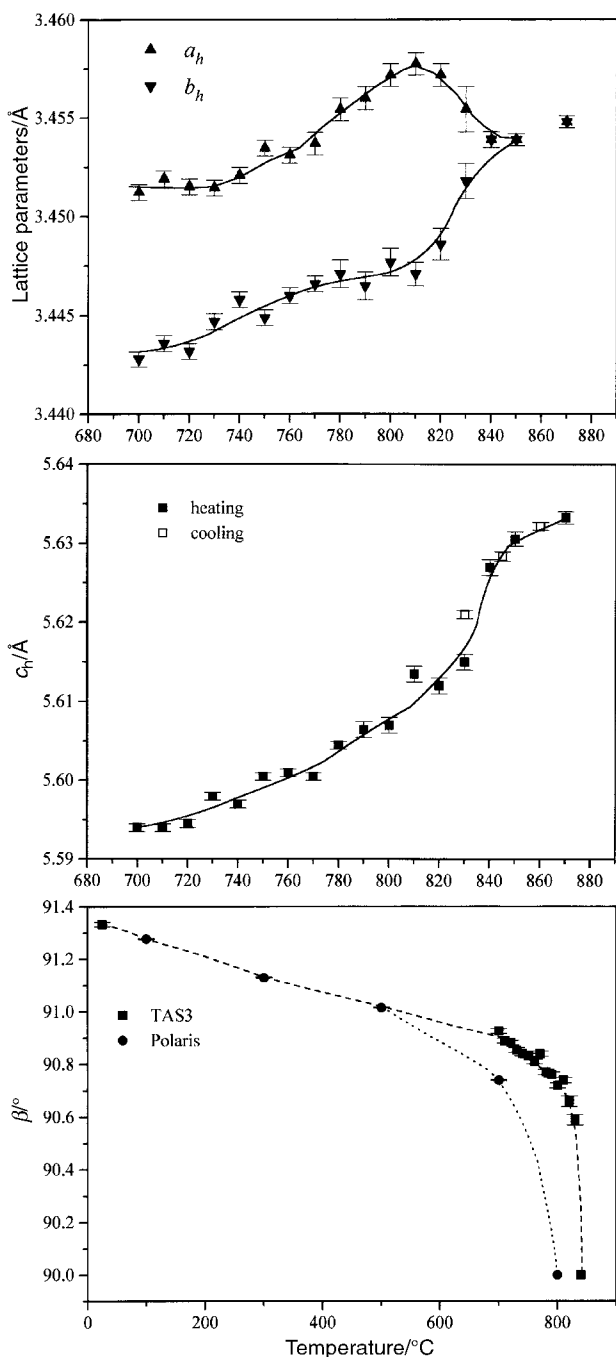


**Fig. 5** The temperature dependence of the unit cell parameters of  $\text{NiCr}_2\text{S}_4$ . To aid comparison, lattice parameters for the monoclinic  $\text{Cr}_3\text{S}_4$  were referred to the hexagonal NiAs unit cell ( $a_m \approx \sqrt{3}a_h$ ,  $b_m \approx b_h$  and  $c_m \approx 2c_h$ ). Lines are a guide to the eye.

of hysteresis. Data collected after cooling the sample to room temperature can be indexed on the basis of the  $\text{Cr}_3\text{S}_4$  unit cell ( $I2/m$ ), and no extra peaks were detected.

## Discussion

As clearly shown by the temperature dependence of the monoclinic angle  $\beta$  (Fig. 5) and the unit cell volume (Fig. 6), the phase transition temperature for the sample investigated on TAS3 is 835(5)°C. Analysis of the diffraction data demonstrated that the high temperature phase exhibits the NiAs structure, with  $P6_3/mmc$  symmetry. This contrasts with the conclusions reached from the time-of-flight experiment, which indicated the same phase change ( $I2/m \rightarrow P6_3/mmc$ ) occurred between 700 and 800°C. However, during the course of the

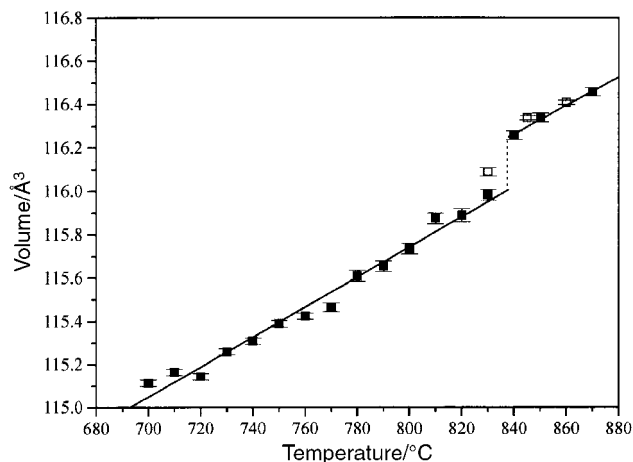


**Fig. 6** The temperature dependence of the unit cell volume per formula unit from data collected on TAS3 on heating (■) and cooling (□). Lines are a guide to the eye.

experiment on Polaris, loss of sulfur was clearly observed leading to a marked increase in the M:S ratio. This suggests that the transition temperature is dependent on the stoichiometry, in agreement with previous studies of analogous systems.<sup>8,9</sup> For example, the order-disorder transition temperature for the  $\text{Cr}_{3 \pm x}\text{Se}_4$  materials shows a parabolic change with composition, having the maximum value at the fully stoichiometric composition.<sup>7</sup> This can be correlated to the defect ordering which originates in the minimisation of the repulsive vacancy-vacancy interaction energy. At the stoichiometric composition  $\text{M}_3\text{S}_4$ , the decrease in energy achieved through the vacancy ordering takes its maximum value, and hence the thermal energy required to disorder the vacancies is higher.

No intermediate structure of the  $\text{CdI}_2$  type was observed, even when data were collected over small temperature increments (10°C). Although powder patterns of the  $\text{CdI}_2$  and NiAs structures are very similar, the possibility of a  $\text{CdI}_2$  type phase being present can be excluded because of the absence of (00 $l$ ) reflections with  $l=2n+1$ . Powder pattern simulations show that for  $\text{NiCr}_2\text{S}_4$  with the  $\text{CdI}_2$  structure, a peak centred at  $d \approx 5.6$  Å should appear; data from the Polaris low angle bank do not exhibit any feature in the range  $5 < d/\text{Å} < 6$ . Moreover, data collected on TAS3 above 830°C do not show any reflections in this region. This contrasts with previous reported transitions in analogous materials, such as  $\text{V}_3\text{S}_4$ ,<sup>4</sup> where  $\text{CdI}_2$  phases were identified. From a statistical thermo-

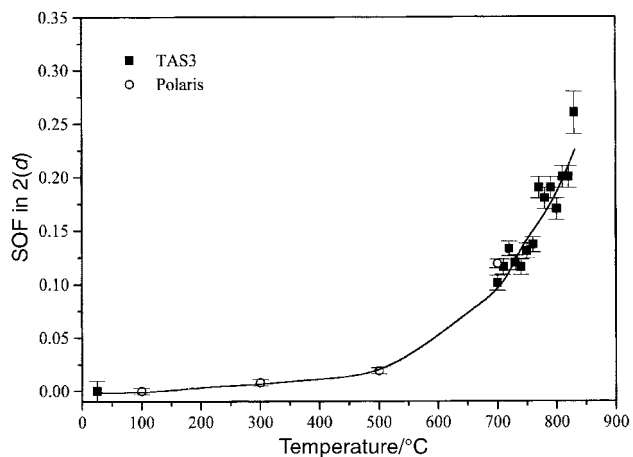


**Fig. 7** Fractional occupancy of the 2( $d$ ) site as a function of temperature. SOF=0.0 corresponds to the ideal  $\text{Cr}_3\text{S}_4$  structure whilst SOF=0.5 corresponds to the  $\text{CdI}_2$  structure. Lines are a guide to the eye.

dynamic treatment,<sup>6</sup> the transition temperature,  $T_c$ , for the CdI<sub>2</sub> to the NiAs phase change for a system M<sub>1-δ</sub>X is given by:

$$T_c = \left( \frac{2(\varepsilon_{vv'} - 3\varepsilon_{vv''})}{k} \right) \delta(1 - \delta) \quad (1)$$

where  $\varepsilon_{vv'}$  is the interaction energy between vacancies perpendicular to the layers and  $\varepsilon_{vv''}$  is the interaction energy between vacancies parallel to the layers. From this expression, it follows that the transition temperature is dependent not only on the composition, but also on the difference between the interlayer and intralayer vacancy–vacancy interaction energies. This implies that for materials with  $\varepsilon_{vv'} \approx \varepsilon_{vv''}$ , the transition temperature tends to zero and hence, for materials which adopt the Cr<sub>3</sub>S<sub>4</sub> structure at room temperature, the CdI<sub>2</sub> structure may never be stabilised. Accordingly, the absence of any intermediate CdI<sub>2</sub> phase for NiCr<sub>2</sub>S<sub>4</sub> stable between the Cr<sub>3</sub>S<sub>4</sub> and the NiAs structure type, may be a consequence of the ratio of the intra- and inter-layer vacancy–vacancy interaction energies. For the systems VS<sub>x</sub> and VSe<sub>x</sub> ( $1.3 \leq x \leq 1.7$ ), Kosuge suggested that the interlayer interaction energy is much higher than the intralayer energy, and therefore, only the CdI<sub>2</sub> phase can be obtained.<sup>5</sup> However, Nakazawa *et al.*<sup>16</sup> reported that in V<sub>5</sub>S<sub>8</sub> both intra- and inter-layer disordering coexist below 800 °C. Above 800 °C, V<sub>5</sub>S<sub>8</sub> transforms to a high temperature phase with a structure intermediate between the NiAs and the CdI<sub>2</sub> type. To our knowledge, no structural refinements have been carried out for the vanadium systems, so the existence of some degree of interlayer disorder cannot be excluded. The high temperature behaviour of the binary vanadium sulfides contrasts with that observed in the ternary sulfide Fe<sub>1.8</sub>V<sub>1.2</sub>S<sub>3.93</sub>, in which both CdI<sub>2</sub> and NiAs phases have been identified at high temperatures.<sup>10</sup> For this material, the transition temperature for the Cr<sub>3</sub>S<sub>4</sub> structure to CdI<sub>2</sub> is 850 °C and the transition temperature to the NiAs phase is 930 °C. This suggests that the relative stability of the NiAs and CdI<sub>2</sub> phases is dependent on the nature of the transition metal cations present.

Although the intermediate CdI<sub>2</sub> phase was not identified in the powder diffraction patterns, refinements demonstrate that, at temperatures below that at which the Cr<sub>3</sub>S<sub>4</sub> to NiAs transition occurs, there is some partial cation disorder within the vacancy layers. As shown in Fig. 7, the site occupancy factor in the 2(*d*) octahedral site, which is empty in the perfectly ordered Cr<sub>3</sub>S<sub>4</sub> structure, increases with temperature, reaching a value of *ca.* 30% at 830 °C. Above the transition temperature, all octahedral sites are equivalent and have an occupancy of 75%.

Data from the Polaris experiment, in which the sample was contained in a standard vanadium can, initially suggested that the phase transition is irreversible. Similarly, a previous study on order–disorder transitions in ternary chalcogenides of titanium reported that the transformation to the NiAs disordered phase is not reversible, and occurs only when the stoichiometry departs from MTi<sub>2</sub>S<sub>4</sub> due to sulfur loss.<sup>17</sup> However, when the experiment was carried out using a sealed sample container, no loss of sulfur was observed and the transformation to the NiAs phase was indeed found to be reversible.

In the room temperature structure, nickel cations occupy sites almost exclusively within the vacancy layer whereas chromium resides in sites in the fully occupied layer. The

magnetic properties of NiCr<sub>2</sub>S<sub>4</sub> may be rationalised in terms of the Goodenough<sup>18</sup> and Kanamori<sup>19</sup> rules by considering only Ni–Ni and Cr–Cr intralayer interactions and Ni–Cr interlayer interactions. Transition to a NiAs phase involves a redistribution of cations between layers such that Ni and Cr cations are randomly distributed over all octahedral sites. This randomness introduces additional, short-range cation–cation interactions. These are likely to be the cause of the magnetic history dependence observed in samples prepared by quenching from high temperatures as this produces a greater degree of disorder than is present in a material prepared by slow cooling.

It can be concluded that NiCr<sub>2</sub>S<sub>4</sub> exhibits an order–disorder transition at 835(5) °C. The high temperature phase has a cation-deficient NiAs structure in which Ni and Cr are statistically distributed between all available octahedral sites. The phase transition is reversible, is accompanied by a discontinuity in the volume and exhibits hysteresis. It is therefore a first order transition.

## Acknowledgements

We wish to thank the EPSRC for a research grant in support of our neutron scattering programme. We acknowledge the financial support of the EC-TMR programme for access to large scale facilities. One of the authors (P.V.) thanks The Leverhulme Trust for a research fellowship.

## References

- 1 A. V. Powell, D. C. Colgan and P. Vaquero, *J. Mater. Chem.*, 1999, **9**, 485.
- 2 A. V. Powell, D. C. Colgan and C. Ritter, *J. Solid State Chem.*, 1999, **143**, 163.
- 3 D. C. Colgan and A. V. Powell, *J. Mater. Chem.*, 1997, **7**, 2433.
- 4 Y. Oka, K. Kosuge and S. Kachi, *J. Solid State Chem.*, 1978, **23**, 11.
- 5 Y. Oka, K. Kosuge and S. Kachi, *J. Solid State Chem.*, 1978, **24**, 41.
- 6 K. Kosuge, in *Chemistry of Non-Stoichiometric Compounds*, Oxford University Press, Oxford, 1993.
- 7 T. Ohtani, R. Fujimoto, H. Yoshinaga and M. Nakahira, *J. Solid State Chem.*, 1982, **48**, 161.
- 8 N. Ohtsuka, K. Kosuge, N. Nakayama, Y. Ueda and S. Kachi, *J. Solid State Chem.*, 1982, **45**, 411.
- 9 Y. Oka, K. Kosuge and S. Kachi, *Mater. Res. Bull.*, 1980, **15**, 521.
- 10 H. Wada, *Bull. Chem. Soc. Jpn.*, 1979, **52**, 2918.
- 11 P. Vaquero, A. V. Powell and B. Lebech, *Physica B*, in press.
- 12 F. Jelinek, *Acta Crystallogr.*, 1957, **10**, 620.
- 13 A. V. Powell, D. C. Colgan and C. Ritter, *J. Solid State Chem.*, 1997, **134**, 110.
- 14 W. I. F. David, M. W. Johnson, K. J. Knowles, C. M. Moreton-Smith, G. D. Crosbie, E. P. Campbell, S. P. Graham and J. S. Lyall, Rutherford Appleton Laboratory Report, RAL-86-102, 1986.
- 15 A. C. Larson and R. B. von Dreele, *General Structure Analysis System*, Los Alamos Laboratory, [Report LAUR 85-748], 1994.
- 16 H. Nakazawa, M. Saeki and M. Nakahira, *J. Less-Common Met.*, 1975, **40**, 57.
- 17 R. H. Plovnick, M. Vlasse and A. Wold, *Inorg. Chem.*, 1968, **7**, 127.
- 18 J. B. Goodenough, in *Magnetism and the Chemical Bond*, Wiley, New York, 1963.
- 19 J. Kanamori, *J. Phys. Chem. Solids*, 1959, **10**, 87.